Draft Survey Based on Image Processing

Wang Zhang, Ying Li and Wenhai Xu
Information Science and Technology College, Dalian Maritime University, Linghai Road, Dalian, China
{zhangwang, ly_123, xuwenhai}@dlmu.edu.cn

Keywords: Draft survey, climbing robot, image processing, neural network, color image segmentation.

Abstract: A draft survey system based on digital image acquisition and processing was designed and implemented to overcome the shortcomings in the conventional manual reading method. The method of draft image acquisition using the climbing robot as a carrier for the network camera was proposed. While climbing along the complex surfaces of the hull under the control of a tablet, the robot could be assigned to shoot the draft and continuously capture high-definition images covering several wave periods. The images were first preprocessed morphologically, and the draft character was then identified by the neural network algorithm so as to numerically represent the draft. Meanwhile, the draft line was identified by using the color image segmentation algorithm. By doing so, the interference of fake waterline caused by the infiltration of waves was successively eliminated, so as to accurately locate the draft line. Field experiments showed that determining the ship's draft by comparing the relative locations of the draft line on the numerically represented draft could achieve a final identification accuracy of 1mm for the detected values, significantly higher than that of 5mm by manual reading.

1 INTRODUCTION

Draft survey is an internationally accepted approach for the cargo transfer of water transport. It is mainly used for weighting bulk cargoes, such as coals, which are at low price and difficult to weight by instruments. Based on the Archimedes' principle, draft survey takes the ship itself as the measuring tool and calculates the hull displacement by measuring the ship draft. Then the cargo weight can be calculated by combining the parameters, such as level of ballast water and port water density, and referring to the "Hydrostatic Data Table" (Liu, Zhang, Sun and Yin, 2014). Conventionally, draft survey is performed by reading the ship's draft on the draft marks, which usually needs to be done by professionals. Since the weather conditions at the arrival of a ship may not be constant, and the draft survey must be conducted immediately after arrival to ensure the subsequent loading and unloading operations. The results are susceptible to wind, waves and subjective factors. It is also impossible for later inspection.

In this paper, to address the problems of manual reading, a draft survey system based on image acquisition and processing was designed and implemented. In the system, the draft images were captured by the climbing robot that carried network HD camera, and the close-up imaging of the marks near the draft line ensures the quality of the materials for image processing. The draft was determined by the draft numerical representation algorithm based on neural network and the draft line identification algorithm based on color image segmentation. Moreover, the integrated analysis of the images covering several wave periods could effectively improve the detection accuracy. At the same time, all relevant data were recorded in the database, guaranteeing later inspection of the measurements and thus avoiding the possible trade-related disputes (Li, Bao and Xu, 2012).

2 SYSTEM COMPOSITION

The draft survey system was divided into an on-site data acquisition sub-system and a back-end data processing sub-system, as shown in Fig. 1. The data acquisition sub-system was composed of the climbing robot, level meter, densitometer, and tablet computer. Under the control of the tablet, it could capture the draft images, measure the level of ballast water and the port water density, and upload data to the server via 4G network. The data processing sub-

Zhang, W., Li, Y. and Xu, W.
Draft Survey Based on Image Processing.
In *3rd International Conference on Electromechanical Control Technology and Transportation (ICECTT 2018)*, pages 642-647
ISBN: 978-989-758-312-4

system centered on the programs of draft numerical representation, draft line identification, load calculation, and database application running on the server. It received the draft images sent by the tablet, calculated the ship's load, and returned it to the tablet for the operator while backing up in the database for later inspection.

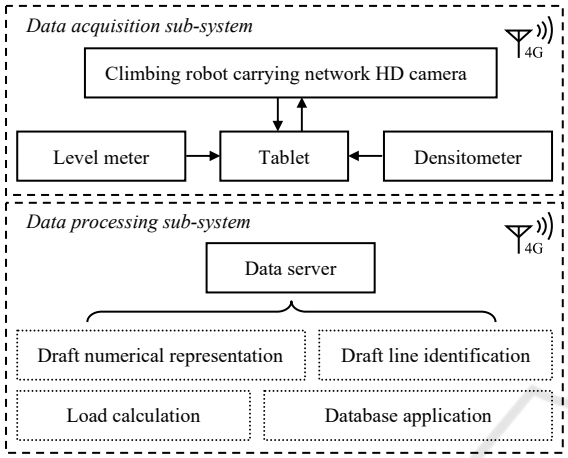

Figure 1: Composition of draft survey system.

3 DRAFT IMAGE PROCESSING

A typical draft image uploaded by the data acquisition sub-system to the data processing sub-system is shown in Fig. 2. The operator could drop the robot at any point from the ship's sides and control the robot to climb on the hull with the tablet. According to the real-time view sent by the camera, the acquisition of draft images could be done even for the non-visible areas.

Figure 2: The draft image of bulk carrier An** captured by the climbing robot.

3.1 Numerical Representation of Draft

The original draft images captured by the camera are not suitable for the numerical representation of the draft. This is mainly due to the fact that most of the original images are subjected to the noises of stains and character distortion caused by shooting angle. What's more, it takes longer to process the larger images. Therefore, the original images must be first transformed into binary ones, and statistical mapping should be plotted vertically to crop the images. Since the draft characters with distinctive white features can form a clear contrast against the background, it will be easy to choose a fixed threshold for turning the images binary after the original images have been transformed into grayscale. The watermark of the camera at the fixed area should be removed from the image and the statistical mapping should be plotted vertically as shown in Fig. 3 (a). As can be seen by comparison, the draft character vertically arranged in the binary image present an obvious stepped increase in their counts in the corresponding mapping. On this basis, it is possible to crop the core area where the draft is located, as shown in Fig. 3 (b).

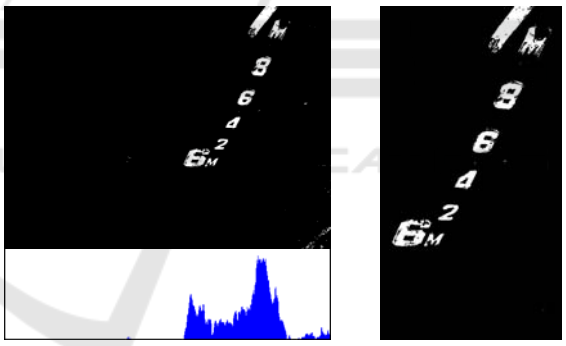

(a) (b)

Figure 3: Preprocessed results of the draft image: (a) vertical statistical mapping of the binary image, (b) the cropped core area.

If there is no obvious noise in an image, the mapping can be then plotted horizontally, in order to crop image of single characters and thus start character identification. However, before that, noise reduction and shear correction of the image could effectively improve the accuracy of subsequent character identification. Given that the characters on the standard metric draft markings contain only the Arabic numerals "0-9" and the capital letter "M", this paper adopted morphology-based noise reduction algorithm. The key operations involved are mathematically described by Eq. (1) and (2):

$$A \circ B = (A \odot B) \oplus B \quad (1)$$

$$A \bullet B = (A \oplus B) \odot B \quad (2)$$

where ∘ denotes opening operation, • denotes closeing operation, ⊙ denotes erosion, and ⊕ denotes dilation. As implied by the combination of erosion and dilation, opening operation can eliminate the small prominences of isolated noise points, thin lines, and edges, while closeing operation can eliminate the internal small holes and curves (Said, Jambek and Sulaiman, 2016). Comparing Fig.3 (b) before processing and Fig.4 (a) after processing, it can be found that the jagged prominences of edges of the characters are noticeably eliminated, and the noises caused by a few large stains can be removed in further character cropping.

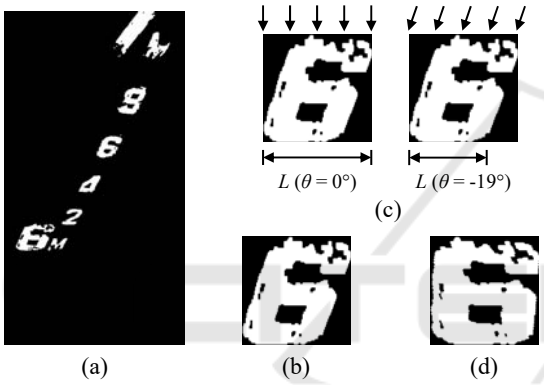

Figure 4: Preprocessed results of the draft image: (a) image after noise reduction, (b) the cropped character, (c) mapping of the character image in different directions, and (d) the character image after shear correction.

The majority of the cropped characters would still be deformed, because of the shooting angle of the robot, as shown in Fig.4 (b). Since it could be difficult for the robot to maintain a stable stance on the raised draft characters, images could only be taken from the diagonal tops of the characters. As a result, the draft characters in an image would inevitably be sheared horizontally. The angle of shear-warp can be extracted by using the mapping method shown in Fig.4 (c), that is, when the mapping angle θ is equal to the shear-warp angle, the mapping length L can be the minimum (Liu, 2017). Let the coordinates of a pixel point in the image be $P(x, y)$, after the shear correction by using affine transformation, the coordinates $P'(x', y')$ can be expressed as follows:

$$\begin{bmatrix} x' \\ y' \\ 1 \end{bmatrix} = \begin{bmatrix} 1 & 0 & 0 \\ \tan\theta & 1 & 0 \\ 0 & 0 & 1 \end{bmatrix} \begin{bmatrix} x \\ y \\ 1 \end{bmatrix} \quad (3)$$

The correction is performed using a bilinear interpolation method. The output pixel value is the average of a 2×2 field samples in the input image, as shown in Fig.4 (d).

Among many of the draft character identification methods that have been tried, the template matching and the neural network algorithms are considered to be effective (Ran and Peng, 2012). The former often uses simple features for comparison, so the algorithm can be conveniently implemented; but the characters like “6”, “8”, and “9” that are morphologically similar are poorly distinguished, especially if the characters are defaced by sea water erosion. The latter identifies the character by the weights of various features, resulting in higher identification accuracy, and its complex algorithm is affordable for high-performance servers (Kim and Xie, 2015).

The typical BP-neural network used in this paper consists of three layers: input, hidden, and output layers. Neurons in adjacent layers are connected to each other, while neurons in the same layer are not connected. As shown in Fig.5, the neural network’s inputs are $x_1, x_2, \ldots, x_i, \ldots, x_N$; the hidden layer’s outputs are $y_1, y_2, \ldots, y_j, \ldots, y_L$; the neural network’s outputs are $o_1, o_2, \ldots, o_k, \ldots, o_M$; the weight from input layer to hidden layer is v_{ij}; the weight from hidden layer to output layer is w_{jk}. For neuron outputs at the hidden and output layers, there is:

$$y_j = f(net_j) = f\left(\sum_{i=1}^{N} v_{ij} x_i\right) \quad (4)$$

$$o_k = f(net_k) = f\left(\sum_{j=1}^{L} w_{jk} y_j\right) \quad (5)$$

The commonly used unipolar Sigmoid function $f(x) = \frac{1}{1+e^{-x}}$ is selected as the activation function. According to the specific needs of draft character identification, the input layer contains 93 neurons, covering various parameters such as the character’ contour, projection, and discrete Fourier features. The output layer contains 11 neurons, corresponding to the numbers “0-9” and the letter “M”, respectively. The hidden layer contains 48 neurons and connects the input and output layers via the full connection, in order to achieve the forward transmission of information and the backward transmission of error. When the output results generated by the input

feature parameters do not match the expected values, the error will be transmitted backwards. Moreover, the weight between layers will be adjusted in a gradient descent manner, until the correct output results are obtained after repeated attempts, thus forming a widely applicable structure of neural network.

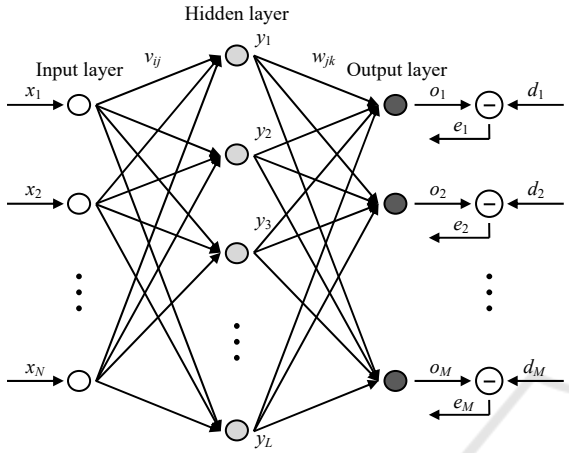

Figure 5: The structure of neural network used for character identification.

3.2 Identification of Draft Line

The key to draft line identification is how to accurately identify the intersection between the hull and the water surface. Drawing on the previous experience of edge detection, the effects of various edge detection operators such as Sobel, Reborts, Log, Zerocross, Canny, and Susan were compared in the experiment (Yu and Zhang, 2015). Among them, operators Sobel and Reborts can digitally approximate the first derivative to extract the edges, but a lot of noises may be left in the processed image. Operators Log and Zerocross use the filtering function to carry out convolution of the image. Compared to operators Sobel and Reborts, they are effective in smoothing the image, but double edges are easily generated as well. The difficulty in applying operator Canny lies in how to determine the size and threshold of Gaussian filter, while the fixed Gaussian filter can hardly detect the edge structures of different scales. Operator Susan has a strong anti-noise capacity, but an appropriate threshold is also difficult to select.

In addition, when using conventional edge-detection operators for image processing, there are often two indistinguishable draft lines, especially when the weather is fine. As clearly shown in the original Fig.6 (a), the upper half of character “6” has an area created by undulating infiltration on the hull. The gray values of this area and the non-infiltrated area form a significant discontinuity, even more evident than the difference between them and the water surface. In the practical detection, therefore, it can be tricky to determine which one is the real draft line. Furthermore, the fluctuation of the water surface and the resulting changes in the reflected light may create obvious discontinuity in the gray image, seriously affecting the actual effect of the conventional edge detection operators.

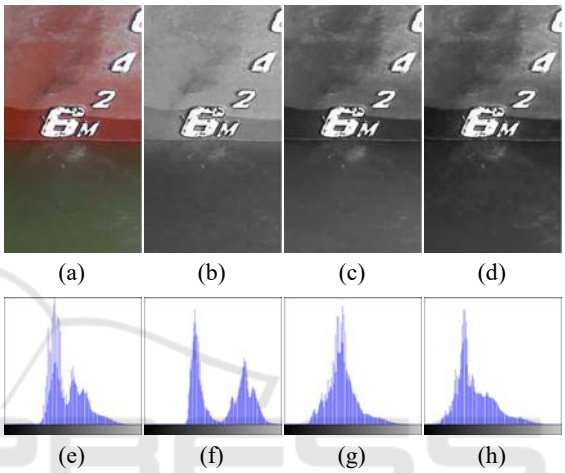

Figure 6: RGB components and their histograms of the draft image: (a) the draft image, (b-d) RGB components, (e) histograms of the draft image, and (f-h) histograms of RGB components.

Given the obvious difference in colors between the hull and the water surface, this paper used the color image segmentation algorithm to achieve the accurate identification of the draft line. As suggested by Fig.6 (e), which is the histogram of Fig.6 (a), the bimodal distributions are caused by the subtle color differences. By extracting the components of R (red), G (green), and B (blue) of the draft image and comparing their histograms, it can found that the histogram corresponding to the R component presents a significant bimodal distribution, while the other components show the unimodal distribution. The hulls of bulk carriers are always painted bright red, while the water surrounding the cargo terminals is generally muddy. As a result, there can be an evident contrast between the two, leading to a distinctive bimodal distribution of the histogram of R component. Influenced by the unimodal distribution of the other two components, this feature is not obvious in the original image. For this reason, the minimum gray value between the two peaks in the histogram of R

component was taken as the threshold, so as to accurately segment the images. The theoretical basis is that the gray values of the pixels adjacent inside the targets or the background area similar, while those of the pixels between the target and the background are different (Peng, Zhou and Lei, 2017). Therefore, the target and the background correspond to different peaks in the histogram. For the pixel point R (x, y) of R component, the valley T between two peaks in the histogram is selected as the threshold. Then the segmented binary image R_{BW} (x, y) can be expressed as:

$$R_{BW}(x,y)=\begin{cases} a\ , & R(x,y)>T \\ b\ , & R(x,y)\le T \end{cases} \tag{6}$$

where a=1 denotes the target, b=0 denotes the background, that is, the hull and the water surface are segmented in the image.

As shown in Fig.7 (a), in the segmented result obtained from R component, the hull and the water surface show an obvious margin, while the fake waterline formed by wave infiltration on the hull does not leave evident traces. Such effect is mainly due to the little impact generated by the infiltration itself in the image of R component. Meanwhile, the valley between the two peaks on the histogram is taken as the threshold for segmentation, which also helps eliminate the influences caused by the small difference in the gray values of the adjacent pixels inside the target or background. In addition, to improve the adaptability of the image segmentation algorithm, the histograms of different color components can be compared other than the histograms of RGB components.

(a) (b) (c) (d)

Figure 7: Identified results of the draft line based on color image segmentation, (a) binary image obtained from R component, (b) pixels on the edges, (c) the detected draft line, and (d) mapping of the draft line in the original image.

The edge pixels in the image are extracted as shown in Fig.7 (b). The details show that although the edge features between the hull and the water surface can be obtained by the above method, the pixels at the edges usually do not fully characterize the edge, especially if the draft line stretches over the draft character. For the edge fractures due to noises and uneven lighting, as well as the other effects of introducing grayscale discontinuities, Hough transform is usually used to assemble the edge pixels into meaningful continuous segments. The basic strategy is as follows: A set of straight lines that pass a specific point in the image are converted to a curve under polar coordinates, the peaks of the curve intersections under polar coordinates are counted in an accumulator, and then the peak corresponds to a straight line with many collinear points in the image (Yan and Yang, 2015). For the identification of the draft line, given that adjusting the climbing robot's location and arm can provide a better shooting angle for the HD camera, the location of the draft line is limited within the lower half of the image, and the angle of the draft line is limited to ±15°. This not only facilitates reducing the interference in the image, but also accelerates the processing speed of Hough transform, as shown in Fig.7 (c). Finally, the resulting line can be remapped to the corresponding location in the original image as the draft line, as shown in Fig.7 (d).

3.2 Calculation of Draft Value

After numerical representation of the draft and locating of the draft line, the draft value can be obtained immediately by comparing the relative location of the two, but one of the details will make a difference in the identification accuracy. Since there is an angle between the camera and the draft, the distances may differ between the numerically represented draft characters. Hence, it is necessary to determine the variation pattern through the fitting approach, and thus the depth value represented by the distance between the draft line and the last character. Considering that Hough transform is used in identifying the draft line, and that the draft line is located by many edge pixels, a locating accuracy at sub-pixel level could be achieved theoretically. Accordingly, the calculation accuracy of the draft value reaches 1mm, significantly higher than the 5mm achieved by manual reading.

4 CONCLUSIONS

Draft survey based on digital image acquisition and processing is an innovative approach that uses pioneering technologies to overcome the inherent

disadvantages of conventional manual reading. The climbing robot that carries the camera to capture images makes it possible to obtain the close-up images of the draft. The robot can climb along the hull under the control of a tablet, and continuously captures several HD images when approaching the draft. The identification algorithm based on neural network and color image segmentation ensures the accurate identification of the draft, with a calculation accuracy of 1mm for draft values in the image. In particular, by combining several draft images, the calculated results could effectively reduce the impacts of wave undulation. Moreover, the entire measurement process could be recorded in the database, guaranteeing later inspection of the measurements and thus avoiding the possible trade-related disputes.

REFERENCES

Liu, C.L., Zhang, X.F., Sun, X.F. and Yin, Y., 2014. Improved draft survey method based on densified table of offsets. Journal of Traffic and Transportation Engineering, 14(3): pp.58-64.

Li, H.X., Bao, Y.F. and Xu, Z. Y., 2012. The research on the risk evaluation and management system for draft survey. Journal of Inspection and Quarantine, 22(4): pp.4-7.

Said, K.A.M., Jambek, A.B. and Sulaiman, N., 2016. A study of image processing using morphological opening and closing processes. International Journal of Control Theory & Applications, 9(31): pp.15-21.

Liu, L.L., 2017. Research on image segmentation technology for a license plate recognition. Bulletin of Science and Technology, 33(4): pp.125-129.

Ran, X. and Peng, J.H., 2012. Ship draft mark recognition based on Image Processing. Journal of Shanghai Maritime University, 33(2): pp.6-9.

Kim, I.J. and Xie, X.H., 2015. Handwritten Hangul recognition using deep convolutional neural networks. International Journal on Document Analysis and Recognition, 8(1): pp.1-13.

Yu, J.D. and Zhang, X.M., 2015. Edge detection algorithm for lines on microscopic image. Optics and Precision Engineering, 23(1): pp.271-281.

Peng, H.，Zhou, X.Z. and Lei, Y.J., 2017. Color image segmentation based on prior color covariance constraint. Computer Engineering, 43(4): pp.251-256.

Yan, H.R. and Yang, M.S., 2015. Line extraction based on improved Hough transform. Infrared Technology, 37(11): pp.970-975.